Membrane Interactions and Metal Ion Effects on Bilayer Permeation of the Lipophilic Ion Modulator DP-109†

Sofiya Kolusheva,‡ Jonathan Friedman,§ Itzchak Angel,§ and Raz Jelinek*,‡

Department of Chemistry, Ben Gurion University, Beer Sheva 84105, Israel, and D-Pharm Ltd., Rehovot 76100, Israel

Received April 19, 2005; Revised Manuscript Received June 17, 2005

ABSTRACT: DP-109, a lipophilic bivalent metal ion modulator currently under preclinical development for neurodegenerative disorders, was designed to have membrane-associated activity, thereby restricting its action to the vicinity of cell membranes. We describe the application of a colorimetric phospholipid/polydiacetylene (PDA) biomimetic membrane assay in elucidating DP-109 membrane interactions and penetration into lipid bilayers. In this membrane model, visible quantifiable color changes were monitored in studying membrane interactions. The colorimetric data identified a biphasic concentration-dependent interaction, with a break point around the critical micelle concentration (CMC) of DP-109. The kinetics and colorimetric dose−response profile of DP-109 indicate that the compound inserts into the lipid bilayers rather than being localized at the bilayer surface. Analysis of interactions of DP-109 with phospholipid/PDA vesicles in which ionic gradients were imposed indicates that membrane activity of DP-109 is strongly affected by electrochemical gradients imposed by K^+ and Zn^{2+}. The ionic gradient effects suggest that the insertion of DP-109 into the membrane may depend on the membrane potential.

Ion modulation has recently been shown to be a prominent factor in varied neuropathologies and neurodegenerative diseases (*1*, *2*). DP-109 [1,2-bis(2-aminophenyloxy)ethane-*N*,*N*,*N*′,*N*′-bis(2-octadecyloxyethyl)ester, *N*,*N*′-disodium salt] is a synthetic lipid analogue of the known metal ion chelator BAPTA (*3*, *4*) (Figure 1). The molecule was designed to modify activities of metal ions such as copper, zinc, calcium, and iron in lipid membrane environments, and was shown to be effective in different models of neurodegeneration (*5*). Moreover, DP-109 (5 mg/kg, per os) administered daily for 3 months has reduced amyloid pathology in the brains of human β-amyloid precursor protein transgenic mice (*6*).

The goal of this study was to investigate the interactions and incorporation of DP-109 into lipid bilayers and to evaluate the impact of metal ions and ionic gradients on its membrane interaction and permeation. Analysis of membrane interactions of DP-109 was carried out here using the newly developed colorimetric phospholipid/polydiacetylene (PDA)[1] vesicle assay (*7*−*12*). The lipid/PDA assay quantifies the blue-to-red transitions induced by membrane-active compounds in solutions of mixed vesicles composed of membrane phospholipids and PDA, mimicking membrane environments (*12*). In particular, the lipid/PDA vesicles exhibit organized bilayer structures, a fundamental feature of the cellular membrane (*12*). The colorimetric transitions in the biomimetic system are ascribed to interactions of the tested compounds with the phospholipid bilayers (*11*, *13*−*15*).

The color transitions of PDA in mixed lipid/polymer assemblies have been attributed to conformational transitions in the conjugated (ene-yne) PDA backbone, induced by structural perturbations in the lipid domains (*7*, *11*, *12*). In particular, several studies have correlated the degree and kinetic properties of the color transitions induced by various biological compounds with the mechanism of insertion into the lipid bilayer (*13*−*16*). The phospholipid/PDA assay has been previously used to analyze diverse membrane processes, including the membrane activity of amyloid peptides (*13*), ligand−receptor interactions (*14*), bilayer insertion of penetration enhancers (*15*), ion transport (*16*), membrane interactions with antimicrobial peptides (*17*), and others.

The experiments reported here compared the membrane action of DP-109 to that of other BAPTA derivatives, and further investigated the effect of lipid composition on membrane interactions of the molecule. The assay was also applied for analysis of membrane interactions of DP-109. The colorimetric dose−response curves reflected, for example, the distinct effect of the critical micelle concentration (CMC) of DP-109 upon bilayer binding. Experiments were designed to examine the extent of lipid surface interactions and bilayer insertion of the compound. The data revealed that membrane interactions of DP-109 depend on the existence of ion gradients by specific monovalent and divalent metal ions, emphasizing the importance of membrane potential on DP-109−bilayer interactions.

EXPERIMENTAL PROCEDURES

Materials. Dimyristoylphosphatidylcholine (DMPC), dimyristoylphosphatidylserine (DMPS), and cholesterol

† R.J. is a member of the Reimund Staedler Minerva Center for Mesoscopic Macromolecular Engineering, funded through the BMBF.

* To whom correspondence should be addressed. Telephone: +972-8-6461747. Fax: +972-8-6472943. E-mail: razj@bgu.ac.il.

‡ Ben Gurion University.

§ D-Pharm Ltd.

[1] Abbreviations: CMC, critical micelle concentration; DMPC, dimyristoylphosphatidylcholine; DMPS, dimyristoylphosphatidylserine; DSC, differential scanning calorimetry; NBD-PE, *N*-(7-nitrobenz-2-oxa-1,3-diazol-4-yl)-1,2-dihexadecanoyl-*sn*-glycero-3-phosphoethanolamine; PDA, polydiacetylene; TFE, trifluoroethanol.

10.1021/bi050718x CCC: $30.25
Published on Web 08/18/2005

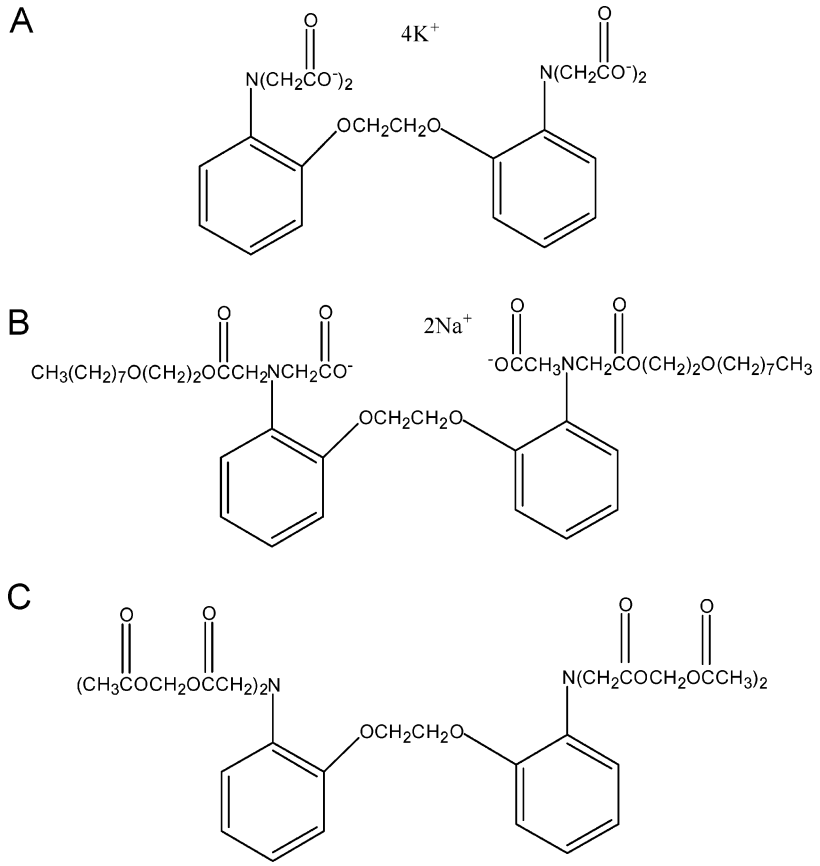

FIGURE 1: Structures of (A) BAPTA (salts), (B) DP-109, and (C) BAPTA-AM.

were purchased from Sigma (St. Louis, MO). Glycine,*N*,*N*′-[1,2-ethanediylbis(oxy-2,1-phenylene)]bis{*N*-[2-(acetyloxy)-methoxy]-2-oxoethyl}bis[(acetyloxy)methyl]ester (9CI) (BAPTA-AM) was obtained from Calbiochem. Glycine,*N*,*N*′-[1,2-ethanediylbis(oxy-2,1-phenylene)]bis[*N*-(carboxymethyl)-(9CI)] (Na-BAPTA) and DP-109 were prepared at D-Pharm Ltd. The diacetylene monomer 10,12-tricosadiynoic acid was purchased from GFS Chemicals (Powell, OH).

Sample Preparation. DP-109 was diluted in trifluoroethanol (TFE) to concentrations of 40 mg/mL prior to use. The stock solution was diluted in deionized water to obtain final concentrations of 4 and 1 mg/mL, which were used in the experiments. Vesicles containing phospholipids and PDA (2:3 molar ratio) were prepared as follows. The phospholipids and monomer constituents in a chloroform/ethanol (1:1) solution were dried together in vacuo followed by addition of deionized water and probe sonication at 70 °C. Vesicles entrapping salts, i.e., KCl/DMPC/PDA, NaCl/DMPC/PDA, and $ZnSO_4 \cdot 7H_2O$/DMPC/PDA, were prepared by addition of 25 mM KCl, 25 mM NaCl, or 3.75 mM $ZnSO_4 \cdot 7H_2O$ solutions, instead of deionized water, to the lipid/monomer mixture prior to probe sonication. Sucrose/DMPC/PDA and dextrose/DMPC/PDA vesicles were prepared by addition of 49.6 mM sucrose or 6.3 mM dextrose solutions instead of deionized water to the lipid/monomer mixture prior to probe sonicaton. Following sonication, the different vesicle solutions were cooled for a few minutes at room temperature and kept at 4 °C overnight, followed by irradiation at 254 nm for 10−20 s to induce polymerization of the PDA. In experiments in which ionic/osmotic gradients were investigated, small volumes of the vesicles containing ions or sugars were placed in large volumes of aqueous solutions, effectively creating either ionic or osmotic gradients.

Colorimetric Measurements. The different compounds were added to the vesicles (0.5 mM total lipid concentration, in 25 mM Tris-base buffer at pH 8), and total solution volumes were then adjusted to 200 μL with deionized water, dextrose or sucrose solutions (to maintain iso-osmolality), or salt solutions. Recording of visible spectra was carried out at room temperature on a Jena Analytical ELISA reader approximately 30 s after addition of compounds to allow color stabilization.

A quantitative value for the degree of blue-to-red color transition is given by the percentage colorimetric response (%CR), which is defined as (*11*)

$$\%CR = [(PB_0 - PB_I)/PB_0] \times 100$$

where $PB = A_{blue}/(A_{blue} + A_{red})$, where A is the absorbance of either the "blue" component in the UV−vis absorbance spectrum (∼640 nm) or the "red" component (∼500 nm). PB_0 is the initial red:blue ratio of the control sample, and PB_I is the value obtained for the vesicle solution after addition of the experimental compound.

In experiments in which ionic gradients were created, the same osmotic pressures were maintained between the vesicle-enclosed and external solution by addition of the appropriate sugar concentrations to yield equal osmolarity. For example, in experiments designed to examine the effect of a KCl gradient between the interior and exterior of the vesicles, we employed DMPC/PDA vesicles containing 25 mM KCl in a solution with 49.6 mM sucrose.

Differential Scanning Calorimetry (DSC). Vesicle concentrations of 2 mM were used in the experiments. Samples were prepared by adding DP-109 (0.3 mM) to the vesicle solutions. The DSC experiments were performed on a VP-DSC instrument (MicroCal). Distilled water served as a blank. Heating scans were run with a rate of 1.5 °C/min. Data analysis was performed using the software provided by MicroCal (Origin version 6.0).

Fluorescence Quenching. *N*-NBD-PE was dissolved in chloroform, added to the DMPC and tricosadiynoic acid at 1 mol %, and dried together in vacuo before sonication (see Vesicle Preparation, above). Addition of *N*-NBD-PE did not affect the initial blue color of the vesicles or the subsequent color transitions. Samples for the fluorescence experiments were prepared by adding different DP-109 concentrations to vesicle solutions at a total lipid concentration of 0.5 mM and 25 mM Tris-base (pH 8). The quenching reaction was initiated by adding sodium dithionite from a 0.6 M stock solution prepared in 50 mM Tris-base (pH 11) buffer, to a final concentration of 10 mM. The decrease in fluorescence was recorded over the course of 300 s at 28 °C using excitation at 467 nm and emission at 535 nm on an Edinburgh FL920 spectrofluorimeter. The fluorescence decay was calculated as a percentage of the initial fluorescence measured before addition of dithionite.

RESULTS

Bilayer Interactions of DP-109. The levels of membrane interactions and penetration through lipid barriers are fundamental factors affecting the activity of pharmacological compounds. This is particularly the case with DP-109, which was specifically designed to be active in the vicinity of membranes (*5*). Our objective in using the new colorimetric vesicle assay in this study was to characterize the interactions of DP-109 with lipid bilayers and to evaluate the factors contributing to and modifying these interactions.

Initial validation of the colorimetric assay for studying membrane interactions of DP-109 was carried out by examination of the response of the blue DMPC/PDA vesicles to addition of either the lipophilic BAPTA derivative BAPTA-AM or the hydrophilic BAPTA salt (Figure 1). Whereas BAPTA-AM is expected to interact and penetrate into lipid bilayers due to charge neutralization (*18*), the BAPTA salt does not have this capability, being a highly charged molecule.

The dose−response curves in Figure 2 (showing the net color transition induced by the added compound after accounting for the solvent effect) demonstrate a significant difference between the color responses of the vesicles to BAPTA-AM compared and the BAPTA salt. Whereas BAPTA-AM induced a considerable increase in %CR, reaching approximately 50% at a concentration of 2 mM (dashed line in Figure 2), the color transitions induced by the same concentrations of BAPTA salt were negligible (solid line in Figure 2). The blue−red change in phospholipid/PDA systems has been attributed to perturbations of the lipid bilayers, induced by the compounds interacting and/or penetrating the lipid bilayers (*11*−*13*). These perturbations are induced by bilayer-interacting compounds which affect the local structure, longer-range organization, and fluidity of lipid bilayers (*11*−*16*, *19*). Thus, BAPTA-AM clearly

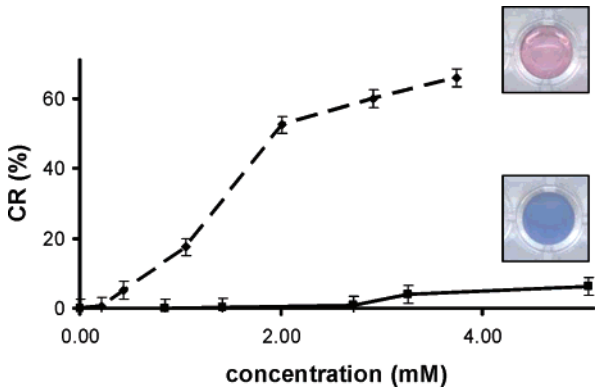

FIGURE 2: Dose−response curves of BAPTA and BAPTA-AM. The curves show the colorimetric response (%CR) of DMPC/PDA vesicles induced by different concentrations in the aqueous vesicle suspension of BAPTA salts (—) and BAPTA-AM (− − −). The pictures depict the maximal colors (highest compound concentrations) of the vesicle suspensions.

perturbs the vesicle bilayers, while the highly hydrophilic BAPTA salt interacted minimally with the vesicles, giving rise to negligible color transitions. Figure 2 demonstrates that the colorimetric vesicle assay is capable of distinguishing between membrane-active and membrane-inactive BAPTA derivatives. Similar evaluation of bilayer activity using the chromatic vesicle system was previously carried out for diverse molecular sets (*13*, *15*, *19*, *20*).

Figure 3 depicts the colorimetric dose−response curve for DP-109, and further presents data acquired by other bioanalytical techniques corroborating the colorimetric analysis. DP-109 was initially dissolved in TFE, diluted in ionized water at different concentrations, and added to 30 μL DMPC/PDA vesicle suspensions prior to acquisition of the visible spectra. It should be noted that the poor solubility of DP-109 in water (~0.01 mg/mL, unpublished data) resulted in the occurrence of aggregation and turbidity in the aqueous vesicle suspensions, particularly at higher concentrations. Efforts to separate water-aggregated and vesicle-bound DP-109 were only partially successful. Accordingly, the concentrations indicated in Figures 3−7 should be interpreted as the total concentrations of DP-109 in water, which include vesicle-bound DP-109, free DP-109 in water, and poorly soluble aggregates.

The dose−response curve of DP-109 (Figure 3) is characterized by two distinct concentration domains separated by a steeper increase in %CR, occurring at approximately 0.5−0.6 mM. Previous colorimetric studies have identified the critical micelle concentration (CMC) of detergent molecules through a similar abrupt increase in the colorimetric dose−response curve (*15*). Accordingly, the steep increase in %CR shown in Figure 3 has been ascribed to the CMC of DP-109. This conclusion is supported by fluorescence quenching experiments (Figure 3C; see below). Since the CMC of DP-109 is around 50 μM, the change in the colorimetric response indicates that a nominal concentration of nonaggregated DP-109 approaches 10% of the total concentration in solution.

Figure 3B depicts the differential scanning calorimetry (DSC) profiles of the DMPC/PDA vesicles (2 mM) before and after addition of DP-109 (0.3 mM). The DSC analysis facilitates evaluation of the effects of DP-109 on the organization and cooperativity properties of both lipid and polymer domains within the vesicles (*12*). The control

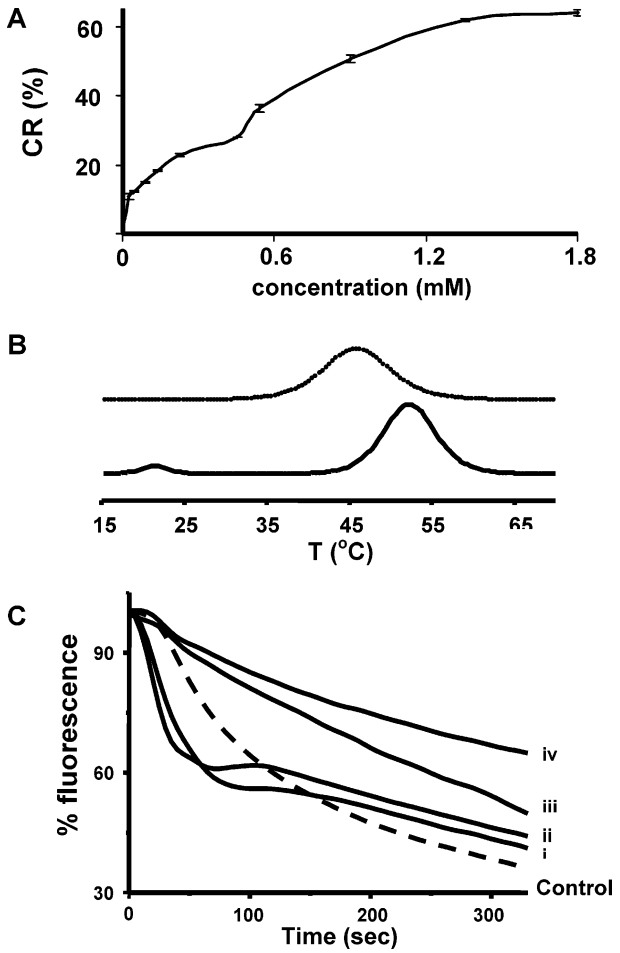

FIGURE 3: (A) Dose−response curve of DP-109 (mean ± standard deviation). The relationship between the colorimetric response (%CR) induced in a DMPC/PDA vesicle solution and the concentration of DP-109. (B) DSC traces. Thermogram of the as-prepared DMPC/PDA vesicle suspension (bottom) and that following addition of DP-109 (top). (C) Fluorescence quenching experiments. Time-decay fluorescence emission curves (535 nm) of NBD-PE incorporated within the DMPC/PDA vesicles after addition of DP-109 at different concentrations. Time zero is defined as the point when sodium dithionite was added: (i) 0.3, (ii) 0.5, (iii) 0.75, and (iv) 1.25 mM DP-109 added.

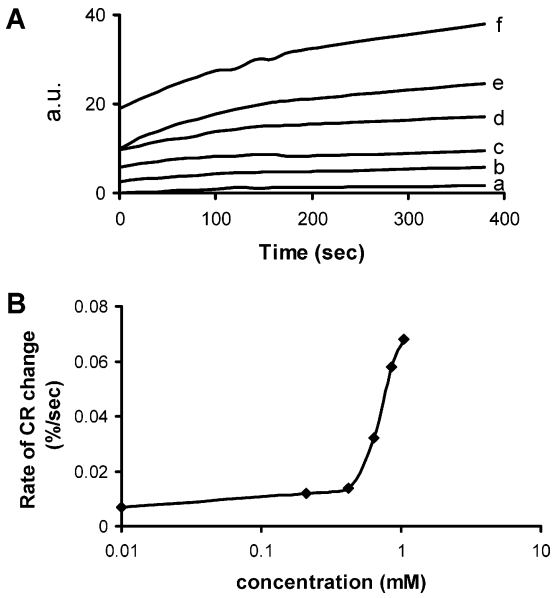

FIGURE 4: (A) Time evolution of the colorimetric transitions of DP-109. The sigmoidal curves depict the time dependence of the intensity of the spectral peak at 500 nm of DMPC/PDA vesicle suspensions into which DP-109 was added at different concentrations: (a) control suspension with no DP-109 added and (b) 0.2, (c) 0.4, (d) 0.6, (e) 0.85, and (f) 1.1 mM DP-109 added. (B) Rates of time-evolution curves. Slopes of the kinetic curves shown in panel A, assuming a linear increase within the first 75 s.

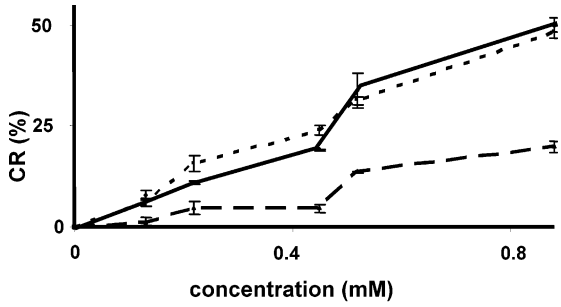

FIGURE 5: Dose−response curves of DP-109 added to different vesicles. The relationship between DP-109 concentration and the colorimetric response (%CR) induced in suspensions of vesicles having different compositions: (—) DMPC/PDA (2:3 mole ratio), (- - -) DMPS/DMPC/PDA (1:1:3 mole ratio), and (— — —) cholesterol/DMPC/PDA (1:1:3 mole ratio).

DMPC/PDA vesicle suspension (Figure 3B, bold spectrum) exhibits the typical highly cooperative phase transition of DMPC (at approximately 23 °C) and PDA (around 53 °C) (*12*). The DSC thermogram recorded after addition of DP-109 clearly demonstrates that the compound induced a significant effect on the phase transitions (Figure 3B, dotted spectrum). Particularly dramatic is the complete disappearance of the DMPC peak following addition of DP-109, indicating a substantial reduction in the degree of molecular ordering within the DMPC domains in the vesicles. The PDA transition is also affected following interaction of DP-109 with the vesicles; however, the consequence here appears as broadening and a shift to a lower temperature (Figure 3B).

Figure 3C presents fluorescence quenching data providing further insight into binding and interactions of DP-109 with the DMPC/PDA bilayers, particularly the putative CMC observed in the colorimetric dose−response curve (Figure 3A). The experiments depicted in Figure 3C measure the fluorescence quenching by soluble sodium dithionite of the phospholipid derivative NBD-PE, additionally incorporated within the DMPC/PDA vesicles. The fluorescent NBD moieties are exposed at the headgroup region of the phospholipid bilayers; accordingly, the experiment depicted in Figure 3C essentially probes molecular interactions and perturbations occurring at the vesicle surface.

The fluorescence quenching experiment yields two important observations. First, the data in Figure 3C clearly show that DP-109 interacts strongly with the phospholipid bilayer surface, leading to significant alteration of the fluorescence-decay curve of NBD. Furthermore, a pronounced difference in the fluorescence decays is apparent between DP-109 concentrations below or at the putative CMC (0.3 and 0.5 mM, for curves i and ii, respectively, in Figure 3C) and concentrations above the CMC (0.8 and 1.2 mM, for curves iii and iv, respectively). Specifically, lower concentrations of DP-109 induced very rapid initial quenching, followed by a time domain exhibiting a much lower quenching rate (Figure 3C, curves i and ii), while the higher DP-109

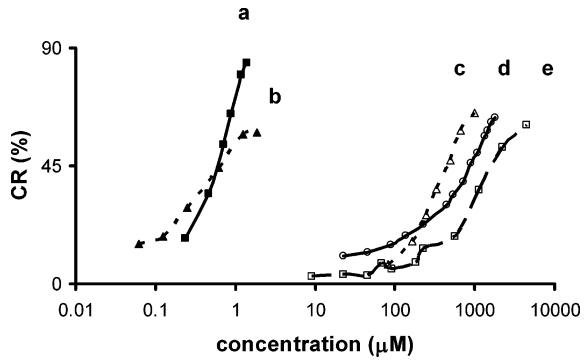

FIGURE 6: Dose−response curves of representative membrane-active compounds and DP-109. Relationships between the colorimetric response (%CR) induced in a DMPC/PDA vesicle suspension and concentrations of (a) histone, (b) cryptdin-4, (c) acebutalol, (d) DP-109, and (e) alamethicin.

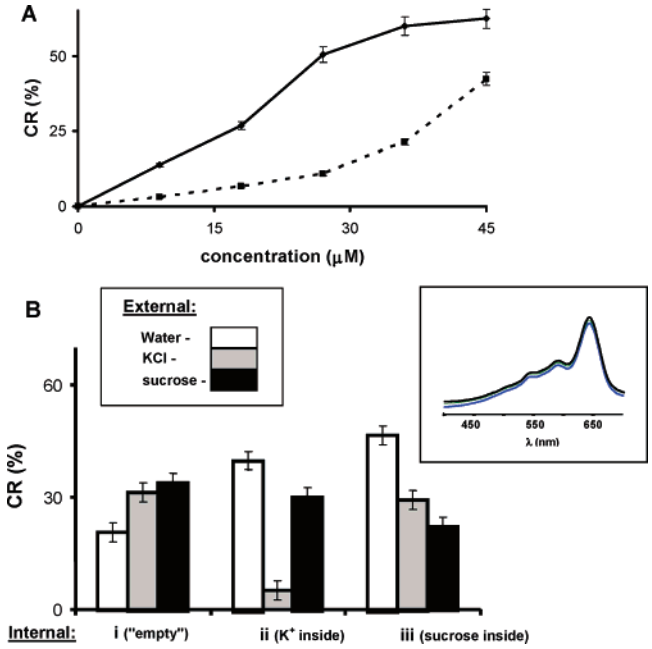

FIGURE 7: K^+ ion gradient effects. (A) Relationship between valinomycin concentration and the colorimetric response (%CR) induced in DMPC/PDA vesicles enclosing 25 mM K^+ ions (—) or DMPC/PDA vesicles enclosing 25 mM Na^+ ions (- - -). (B) Bar diagram depicting the %CR induced by DP-109 (concentration of 0.5 mM) added to vesicle suspensions having different K^+ ion distributions and osmotic pressures: (i) DMPC/PDA vesicles in aqueous suspension, (ii) DMPC/PDA vesicles enclosing 25 mM KCl, and (iii) DMPC/PDA vesicles enclosing 49.63 mM sucrose. White columns depict data for the case in which the external solution of the vesicles was pure water, gray columns for the case in which the external solution contained 25 mM KCl, and black columns for the case in which the external solution contained 49.63 mM sucrose. The inset shows the UV−vis spectra of the different as-prepared vesicle suspensions.

concentrations gave rise to exponential fluorescence decay, albeit weaker quenching than the control (Figure 3C, curves iii and iv).

Kinetic analysis of the color transitions induced by DP-109 in DMPC/PDA vesicles in Tris buffer solutions (Figure 4) complements the dose−response data and supports the interpretation pertaining to the CMC effect. The curves shown in Figure 4 represent the time dependence of the peak at 500 nm (corresponding to the red color of the solution) induced in the vesicle system by specific concentrations of DP-109. For example, at a concentration of 0.2 mM, the initial intensity of the spectral peak at 500 nm induced by DP-109 was approximately 3 [arbitrary units (au)], increasing to 6 au within 350 s (curve b, Figure 4A). However, at a concentration of 0.8 mM (curve e, Figure 4A), the magnitude of the 500 nm peak increased more sharply from 10 au to more than 20 au within the same time span. Importantly, the data in Figure 4A demonstrate the existence of two kinetic domains. At concentrations below and including 0.4 mM, the final color was only marginally higher than the color change induced initially. However, at DP-109 concentrations of $\geq$0.6 mM, a significant and more rapid increase in the blue−red transition was recorded over a period of 6 min.

The differences among the kinetic curves shown in Figure 4A are also reflected in the rate of color change as calculated from the slopes of the curves within the first 75 s, corresponding to the linear phase of the color transitions (Figure 4B). Figure 4B clearly shows that a pronounced rate threshold was observed when the vesicle-bound DP-109 concentrations were higher than the CMC. Like the dose−response curves in Figure 3, this finding points to two distinct interaction profiles for DP-109 with lipid vesicles that depend on the concentration range.

We additionally investigated the interactions of DP-109 with various membrane models using chromatic vesicles with different lipid compositions (Figure 5). The dose−response curves in Figure 5 compare the %CR induced by DP-109 in vesicles containing DMPC and PDA (2:3 mole ratio), DMPC, cholesterol, and PDA (1:1:3), or DMPC, DMPS, and PDA (1:1:3). These compositions were selected for examination of the effects on bilayer interactions of DP-109 with particular lipid membrane components such as cholesterol, an abundant lipid species in mammalian and human plasma membranes, and DMPS, a representative negatively charged phospholipid present in various bilayers, particularly bacterial membranes. Importantly, all three curves exhibit the %CR "step" at approximately 0.5 mM, ascribed to the CMC of DP-109 (Figure 5). However, differences in the overall increase in %CR were apparent among the vesicles. In particular, addition of DP-109 to DMPC and PDA or DMPC, DMPS, and PDA induced similar colorimetric effects, while the %CR induced by DP-109 in the DMPC/cholesterol/PDA vesicle suspension was significantly smaller over the entire concentration range that was examined (Figure 5). For example, at a concentration of approximately 0.5 mM immediately above the CMC, the %CR values calculated in the DMPC/PDA or DMPC/DMPS/PDA vesicle solutions were on the order of 30%, while the same concentration of DP-109 in a DMPC/cholesterol/PDA solution gave rise to a much less pronounced color transition, a %CR of approximately 10% (Figure 5). The reduced colorimetric sensitivity of the cholesterol-containing vesicles most likely corresponds to the higher bilayer rigidity conferred by cholesterol (*12*), consequently decreasing lipid mobility within the vesicles. A similar attenuation of the colorimetric response due to bilayer rigidity following incorporation of cholesterol was observed in previous studies (*20*).

Degree of Bilayer Penetration. An important question relating to the mode of action of lipophilic drug compounds such as DP-109 concerns the degree of bilayer penetration (*21*−*23*). To address this question, we compared the dose−response curves of DP-109 in DMPC/PDA vesicles to similar

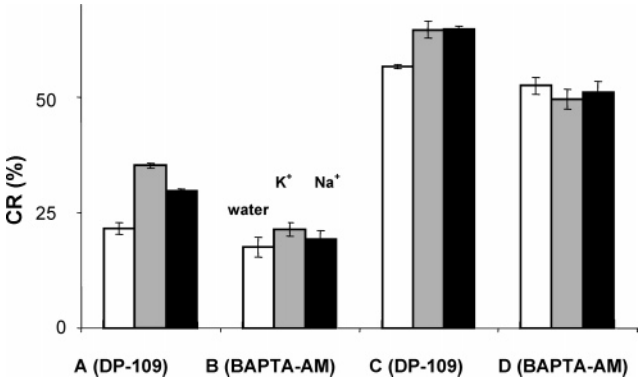

FIGURE 8: K^+ and Na^+ ion gradient effects, with DP-109 and BAPTA-AM. %CR induced by addition of either DP-109 or BAPTA-AM to DMPC/PDA vesicles incorporating no ions (white bars), 25 mM KCl (gray bars), or 25 mM NaCl (black bars): (A) 0.22 mM DP-109 added, (B) 1 mM BAPTA-AM added, (C) 1 mM DP-109 added, and (D) 2 mM BAPTA-AM added.

curves obtained for representative biological and pharmacological standards with known membrane binding properties (Figure 6). Specifically, this figure shows the logarithmic-scale concentration dependence of %CR induced by cryptdin-4 [a short amphipathic antimicrobial peptide (*24*)], histone [a highly positively charged protein (*25*)], acebutalol, a pore-forming anaesthetic drug (*26*), alamethicin, a channel-forming membrane peptide (*27*), and DP-109.

Significantly different concentration ranges of the dose−response curves were observed (Figure 6). Cryptdin-4 (curve b) and histone (curve a), which are expected to bind at the vesicle interface, both induced colorimetric transformations at very low concentrations [the plateaus of high %CR were reached at concentrations of $\leq 1\ \mu$M (Figure 6)]. On the other hand, acebutalol (curve c) and alamethicin (curve e), both lipophilic substances that penetrate into the hydrophobic core of lipid bilayers, required more than order of magnitude greater concentrations, between 10 and 100 μM, to induce color transitions (Figure 6). The dose−response curve of DP-109 (curve d) is in the latter concentration range, between acebutalol and alamethicin. The differences in the concentration ranges in which the blue−red transitions were induced by the different compounds could be explained by the color induction mechanisms in the lipid/PDA vesicles (see the Discussion).

Effects of Monovalent Ions on Membrane Interactions. Electrochemical potentials across membranes generally influence ion fluxes and ligand−receptor interactions (*28*, *29*). Furthermore, ions themselves also modulate the surface potential, which can have an effect on membrane interactions. We applied the colorimetric vesicle assay to investigate the effects of ion gradients on the interactions of DP-109 with lipid bilayers (Figures 7−9). Previous work has demonstrated induction of ion-selective colorimetric responses within phospholipid/PDA vesicles by anchoring ionophores in the phospholipid moieties (*16*). In the study presented here, we have further examined whether the chromatic vesicles could also exhibit specificity toward changes in electrochemical gradients across the lipid−PDA barrier by imposing ionic gradients across the vesicle membranes. The colorimetric responses of DMPC/PDA vesicles encapsulating either K^+ or Na^+ ions following addition of the K^+-selective ionophore valinomycin (*30*) are shown in Figure 7A.

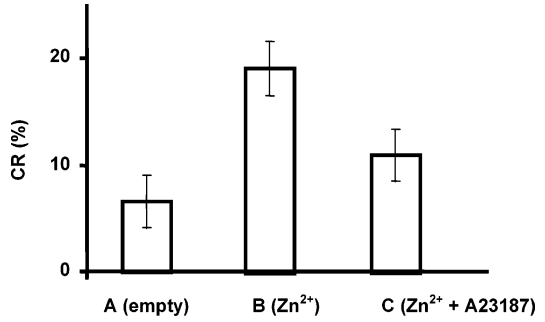

FIGURE 9: Zn^{2+} ion gradient effects. Bar diagram depicting the %CR induced by DP-109 (0.135 mM) added to (A) DMPC/PDA vesicles not containing zinc ions, (B) DMPC/PDA vesicles enclosing Zn^{2+} ions at a concentration of 3.25 mM (the external solution contained 6.32 mM dextrose to equalize the osmotic pressure inside the vesicles), (C) DMPC/PDA vesicles enclosing 3.25 mM Zn^{2+} ions (the external solution contained 6.32 mM dextrose), and also the ionophore A23187 (25 μM). All results are the net colorimetric effects; i.e., the separate transitions induced by the Zn^{2+} ions and ionophore were subtracted from the total observed %CR.

The dose−response curves (Figure 7A) demonstrate that a significantly higher %CR was induced following the addition of valinomycin to the KCl-containing vesicles, compared to a smaller effect when valinomycin was added to vesicles incorporating NaCl. For example, at a valinomycin concentration of 15 μM, a %CR of approximately 20% was recorded in the KCl-DMPC/PDA vesicle solution, while less than 5% was observed for the NaCl-DMPC/PDA vesicles (Figure 7A). The selectivity in the chromatic effect is similarly expressed in the EC_{50} value of 27 μM when valinomycin was added to KCl-DMPC/PDA vesicles compared to approximately 40 μM in case of the NaCl-DMPC/PDA vesicles (Figure 7A).

To further investigate the effect of ionic and osmotic gradients on interactions of DP-109 with membranes, different gradient conditions were imposed on the vesicles. The bar chart (Figure 7B) characterizes the effects of either K^+ or osmotic gradients on membrane interactions of DP-109. Three types of vesicle constructs were examined in the experiment: "conventional" DMPC/PDA vesicles prepared in aqueous solutions (Figure 7B, curve i), DMPC/PDA vesicles enclosing 25 mM KCl (curve ii), and DMPC/PDA vesicles enclosing 49.63 mM sucrose (curve iii). The inclusion of different solutions within the vesicles did not alter their intrinsic structural and colorimetric properties. For example, the inset in Figure 7B demonstrates that the UV−vis spectra of the polymerized blue vesicles were almost identical, indicating a similar degree of polymerization. Transmission electron microscopy analysis (data not shown) additionally pointed to similar vesicle shapes and morphologies.

It should be further emphasized that the %CR values depicted in Figure 7B are the net color changes, calculated by subtracting the separate colorimetric transitions induced by the ions or the sugar from the recorded total %CR. Accordingly, the different column heights in Figure 7B reflect the effects of ionic or osmotic gradients on membrane−DP-109 interactions. First, there appears to be a general increase in color transitions induced by DP-109 when osmotic or ionic gradients were formed, indicating more significant bilayer interactions in such situations. For example, when DP-109 was added to gradient-free DMPC/

PDA vesicles, the %CR was approximately 20% (white bar, Figure 7Bi). However, creation of either an ionic gradient or an osmotic gradient after addition of sucrose resulted in an increase in %CR to more than 30% (gray and black bars, respectively, in Figure 7Bi). Similarly, when DP-109 was placed in pure water solutions and added to vesicles containing a higher concentration of KCl (white column, Figure 7Bii) or vesicles containing sucrose (white column, Figure 7Biii), the colorimetric response increased to approximately 40 or 45%, respectively.

One of the most significant results that is apparent in Figure 7B is the sensitivity of the colorimetric response induced by DP-109 toward a K^+ gradient across the DMPC bilayer. Independent measurements employing a K^+-sensitive fluorescent dye confirmed that K^+ gradients can be created between the vesicle interior and exterior (Supporting Information). The data in Figure 7B indicate an almost negligible color response when DP-109 was added to a DMPC/PDA vesicle suspension having equal KCl concentrations inside and outside of the vesicles (gray bar, Figure 7Bii). This negligible color change stands in striking contrast to the high %CR obtained when DP-109 was added to vesicles in which a higher concentration of K^+ ions existed outside the vesicles (gray bars, Figure 7Bi and -ii) or in which the K^+ concentration inside the vesicles was greater than that in the external solution (white column and black column in Figure 7Bii). Note that this increased colorimetric response occurred when the gradient from the inside out was ionic. Equalizing the osmotic pressures inside and outside the vesicles using sucrose did not significantly reduce the %CR (black column in Figure 7Bii and gray column in Figure 7Biii). The absence of bilayer interactions of DP-109 when K^+ levels were equalized between the vesicle interior and exterior points to a significant dependence of membrane interactions on the existence of a K^+ gradient across the bilayer.

To further verify the role of K^+ membrane potential in determining the activity of DP-109, we compared the chromatic response induced by the compound to the color transitions induced by its lipophilic analogue BAPTA-AM (*31*, *32*) (Figure 8). The bar chart in Figure 8 summarizes the colorimetric responses of DMPC/PDA vesicles following separate additions of DP-109 and BAPTA-AM. The experimental design was aimed at investigating the colorimetric response of the vesicles either without ionic gradients present (white bars) or in solutions containing K^+ (gray bars) or Na^+ (black bars). The concentrations used for the two compounds were selected in an effort to compare similarly induced %CR values before and after reaching the CMC of DP-109 (see Figures 2 and 3).

The data in Figure 8 show that at both concentrations that were examined BAPTA-AM did not exhibit sensitivity to either K^+ or Na^+. Essentially, the color changes induced by 1 mM BAPTA-AM (%CR of approximately 20%, Figure 8B) or 2 mM BAPTA-AM (%CR of 50%, Figure 8D) were not affected by the presence or absence of ionic gradients across the bilayer vesicles. DP-109, on the other hand, demonstrated a considerable sensitivity toward the existence of an ionic gradient. At a low concentration of 0.22 mM, the presence of either 25 mM KCl or 25 mM NaCl in the vesicle solution increased the colorimetric response from around 20% (white bar, Figure 8A) to almost 45% for KCl (gray bar, Figure 8A) or to around 35% for NaCl (black bar, Figure 8A). An ionic effect was also detected when 2 mM DP-109 was added to the vesicles (Figure 8C). The presence of either KCl or NaCl in the external solution increased the %CR induced by DP-109 from approximately 55% (white columns, Figure 8C) to more than 70% (gray or black columns, Figure 8C). Similar evidence of the significant difference between the ion gradient dependence of the colorimetric response of DP-109 and BAPTA-AM has been provided in experiments where the ionic gradient was created inside-out (Supporting Information).

In addition to monitoring the influence of monovalent ions such as K^+ on the action of DP-109, determining the effects of divalent ions, in particular, zinc, which is abundant in physiological systems (*33*, *34*), is important. Zinc is one of the metal ions implicated in several chronic neurodegenerative conditions (*35*). DP-109 as a chelator of bivalent metal ions is understood to have moderate affinity for zinc and acts to prevent interference with normal zinc levels, but concomitantly allows sequestration of excessive zinc ion levels (unpublished data).

The consequences of forming and disrupting an ionic gradient of Zn^{2+} are shown in Figure 9. The data in Figure 9 depict the colorimetric responses induced by 0.135 mM DP-109 interacting with "empty" DMPC/PDA vesicles versus Zn^{2+}-containing vesicles. Like the experiments utilizing K^+ gradients (Figure 7B), UV−vis spectral measurements confirmed that the degree of polymerization (initial blue color) of the Zn^{2+}-containing vesicles was highly similar to that of the Zn^{2+}-free vesicles (data not shown). Comparison of the columns (Figure 9A,B) indicates that creation of a zinc gradient between the vesicle interior and the external solution (while maintaining in the aqueous solution an appropriate concentration of dextrose to ensure iso-osmolarity between the inside and outside of the vesicles) gave rise to an increase in %CR, from approximately 5% without an ionic gradient (Figure 9A) to almost 20% in the presence of a gradient (Figure 9B).

An intriguing result was obtained when the ionophore A23187 (*36*) was co-added to the Zn^{2+}/DMPC/PDA vesicle solution prior to adding DP-109 (Figure 9C). The bar column (Figure 9C) shows that the colorimetric response recorded in the vesicle suspension when A23187 was co-added (%CR of 10%) was lower than in a solution which did not contain the ionophore (%CR of 20%). This result most likely corresponds to the ionophore action in reducing the ionic gradient by transporting the Zn^{2+} ions across the bilayers. As a consequence, the disrupted zinc gradient resulted in the lower bilayer activity of DP-109 (Figure 9C). Overall, the data presented in Figure 9 provide compelling evidence of the ability of zinc gradients to regulate the extent of membrane interactions of DP-109, as for the monovalent ions that have been examined.

DISCUSSION

In this work, we have analyzed membrane interactions of DP-109 and evaluated the dependence of such interactions upon membrane composition and ionic and osmotic gradients using a colorimetric membrane model assay. Colorimetric dose−response curves, which correlated the blue−red transitions within the phospholipid/PDA vesicles to compound concentrations, provided comprehensive information about

the membrane interactions and the degree of membrane penetration by the compound.

Dose−response analysis demonstrated an abrupt increase in membrane affinity of DP-109 occurring around the CMC (Figure 3A). The data indicate that the formation of micellar aggregates promotes bilayer interactions of DP-109. Indeed, micellar aggregates of single-acyl chain compounds such as DP-109 are expected to facilitate stronger membrane perturbations compared to the soluble individual molecules, leading to the %CR "jump" at the CMC. Similar CMC effects in %CR dose−response curves were previously detected for other pharmaceutical compounds (*15*). Application of other bioanalytical techniques (Figure 3B) corroborated this interpretation. In particular, fluorescence quenching experiments that followed reduction of surface-incorporated NBD fluorescence by a soluble quencher featured a significant difference in the quenching profile around the putative CMC. The rapid decrease in NBD fluorescence at lower DP-109 concentrations (Figure 3C) can be ascribed to rapid penetration of the monomers into the phospholipid bilayer. However, formation of micellar aggregates at higher DP-109 concentrations is expected to result in their attachment to the bilayer surface (rather than penetration), leading to "masking" of the fluorescent dye and the reduced quenching observed in Figure 3C (curves iii and iv).

Kinetic analysis of the colorimetric responses (Figure 4) further highlighted the distinct effect of the CMC upon membrane interactions of DP-109. At concentrations below the CMC, minor colorimetric transitions occurred in the vesicle solution following addition of DP-109. However, bilayer perturbations by the larger DP-109 micelles were much more pronounced, leading to faster and more significant colorimetric transitions as compared to those of the soluble individual molecules (below the CMC, Figure 4B). The colorimetric data further demonstrate the dependence of DP-109−bilayer interactions on lipid composition (Figure 5). In particular, the increased rigidity of the lipid bilayer in the presence of cholesterol resulted in a lower level of perturbation by DP-109, most likely due to less penetration of the compound into the bilayer.

The comparison of concentration ranges in which colorimetric changes were induced by DP-109 to those of other substances (Figure 6) yields information about the extent of bilayer penetration. In particular, previous studies have demonstrated that localization of membrane-active compounds at the water−lipid interface (i.e., at the surface region of the phospholipid leaflet) induces the colorimetric transitions at lower concentration ranges compared to molecules penetrating deeper into the bilayer core (*19*). This relationship between the extent of bilayer permeation and the color change is due to the fact that surface perturbations of the pendant side chains of PDA are the primary factors responsible for the blue−red transitions (*17*). According to this structural description, the relative positions of the dose−response curves (Figure 6) are directly related to the extent of penetration into the lipid bilayer. Specifically, molecules that aggregate at the lipid−water interface give rise to stronger perturbations to the PDA side chains, thus inducing the structural transitions of the polymer (and corresponding color change) at a very low concentration range (*24*). On the other hand, acebutalol and alamethicin are known to insert into the hydrophobic cores of lipid bilayers to form pores or channels (*26*, *27*), resulting in the higher concentration range of the %CR dose−response curves shown for these compounds in Figure 6. In light of this description, the proximity of the DP-109 dose−response curve to those of acebutalol and alamethicin points to insertion of the compound into the phospholipid bilayer rather than vesicle surface interactions. This description is consistent with DP-109 structural design, emphasizing the bulky hydrophobic residues (Figure 1B).

An important aspect of this study has been to decipher the relationships between membrane interactions of DP-109 and ionic and osmotic gradients across membrane bilayers. To address these issues, we initially examined the sensitivity of the colorimetric assay toward ionic gradients. Experiments carried out by adding the ionophore valinomycin to vesicles containing different cations (in which ionic gradients exist) confirmed the sensitivity of the colorimetric transitions to the presence of specific ions inside the vesicles. The data in Figure 7A validate the use of the colorimetric assay for studying effects of ionic complexation in bilayer environments, and the existence of ion gradients.

The colorimetric data depicted in Figure 7B provide important insight into the effects of osmotic and ionic gradients upon bilayer interactions of DP-109. The experiments revealed a direct correlation between the extent of membrane interactions of DP-109 and the existence of a K^+ gradient across bilayers. In particular, the minimal bilayer interactions of DP-109 (i.e., very small color change) when K^+ levels were identical inside and outside of the vesicles point to a predominant dependence of membrane interactions of DP-109 on the existence and size of the K^+ gradient.

The dependence of DP-109 upon ionic gradients is particularly revealing when it is compared to its parent chelator compound BAPTA-AM (Figure 8). Whereas DP-109 exhibited enhanced bilayer perturbation activities in the presence of Na^+ or K^+ gradients, no such dependence was detected for BAPTA-AM. This result is consistent with the nonionic character of BAPTA-AM. The dependence upon electrochemical gradients of divalent ions such as zinc upon DP-109−membrane interactions was also apparent (Figure 9). The colorimetric data showed that the existence of an ionic gradient when zinc ions were encapsulated inside the phospholipid/PDA vesicles enhanced the colorimetric response induced by DP-109 (Figure 9B), while disrupting the gradient with a Zn^{2+}-specific ionophore resulted in a lower bilayer activity of DP-109 (Figure 9C). Another possible explanation for the reduced color change is binding of DP-109 to the zinc ions extracted from inside the vesicles by the A23187 ionophore, thereby reducing its extent of bilayer interactions. Overall, the data presented in Figures 7−9 provide compelling evidence of the ability of ionic gradients to regulate membrane interactions of DP-109. This regulation could mean that the interaction of DP-109 with its target cells in the brain could be dependent on the activity of those cells, as reflected by changes in their excitability and ionic gradients.

ACKNOWLEDGMENT

R.J. is a member of the Ilse Katz Center for Nanotechnology.

SUPPORTING INFORMATION AVAILABLE

Evaluation of K^+ gradients and effect of a K^+ gradient from inside-out on the colorimetric response. This material is available free of charge via the Internet at http://pubs.acs.org.

REFERENCES

1. Kaur, D., Yantiri, F., Kumar, J., Mo, J. O., Rajagopalan, S., Viswanath, V., Boonplueang, R., Jacobs, R., Yang, L., Beal, M. F., DiMonte, D., Volitaskis, I., Ellerby, L., Cherny, R. A., Bush, A. I., and Andersen, J. K. (2003) Genetic or Pharmacological Iron Chelation Prevents MPTP−Induced Neurotoxicity In Vivo: A Novel Therapy for Parkinson's Disease, *Neuron 37*, 923−933.
2. Curtain, C. C., Ali, F. E., Smith, D. G., Bush, A. I., Masters, C. L., and Barnham, K. J. (2003) Metal ions, pH and cholesterol regulate the interactions of Alzheimer's disease amyloid-β peptide with membrane lipid, *J. Biol. Chem. 278*, 2977−2982.
3. Tymianski, M. (1995) Neuroprotection in vitro and in vivo by cell membrane-permeant Ca^{2+} chelators, *Clin. Exp. Pharmacol. Physiol. 22*, 299−300.
4. Collatz, M. B., Ruedel, R., and Brinkmeier, H. (1997) Intracellular calcium chelator BAPTA protects cells against toxic calcium overload but also alters physiological calcium responses, *Cell. Calcium 21*, 453−459.
5. Angel, I. B. A., Horovitz, T., Taler, G., Krakovsky, M., Resnitsky, D., et al. (2002) Metal ion chelation in neurodegenerative disorders, *Drug Dev. Res. 56*, 300−309.
6. Lee, J.-Y., Friedman, J. E., Angel, I., Kozak, A., and Koh, J.-Y. (2004) The lipophilic metal chelator DP-109 reduced amyloid pathology in brains of human β-amyloid precursor protein transgenic mice, *Neurobiol. Aging 25*, 1315−1321.
7. Charych, D. H., Nagy, J. O., Spevak, W., and Bednarski, M. D. (1993) Direct colorimetric detection of a receptor−ligand interaction by a polymerized bilayer assembly, *Science 261*, 585−588.
8. Li, Y., Ma, B., Fan, Y., Kong, X., and Li, J. (2002) Electrochemical and Raman studies of the biointeraction between *Escherichia coli* and mannose in polydiacetylene derivative supported on the self-assembled monolayers of octadecanethiol on a gold electrode, *Anal. Chem. 74*, 6349−6354.
9. Gill, I., and Ballesteros, A. (2003) Immunoglobulin-polydiacetylene sol−gel nanocomposites as solid-state chromatic biosensors, *Angew. Chem., Int. Ed. 42*, 3264−3267.
10. Rangin, M., and Basu, A. (2004) Lipopolysaccharide identification with functionalized polydiacetylene liposome sensors, *J. Am. Chem. Soc. 126*, 5038−5039.
11. Okada, S., Peng, S., Spevak, W., and Charych, D. (1998) Color and chromism of polydiacetylene vesicles, *Acc. Chem. Res. 31*, 229−239.
12. Kolusheva, S., Wachtel, E., and Jelinek, R. (2003) Biomimetic lipid/polymer colorimetric membranes: Molecular and cooperative properties, *J. Lipid Res. 44*, 65−71.
13. Porat, Y., Kolusheva, S., Jelinek, R., and Gazit, E. (2003) The Human Islet Amyloid Polypeptide Forms Transient Membrane-Active Prefibrillar Assemblies, *Biochemistry 42*, 10971−10977.
14. Kolusheva, S., Kafri, R., Katz, M., and Jelinek, R. (2001) Rapid colorimetric detection of antibody-epitope recognition at a biomimetic membrane interface, *J. Am. Chem. Soc. 123*, 417−422.
15. Evrard, D., Touitou, E., Kolusheva, S., Fishov, Y., and Jelinek, R. (2001) A new colorimetric assay for studying and rapid screening of membrane penetration enhancers, *Pharm. Res. 18*, 943−949.
16. Kolusheva, S., Shahal, T., and Jelinek, R. (2000) Cation-Selective Color Sensors Composed of Ionophore-Phospholipid-Polydiacetylene Mixed Vesicles, *J. Am. Chem. Soc. 122*, 776−780.
17. Kolusheva, S., Shahal, T., and Jelinek, R. (2000) Peptide-membrane interactions studied by a new phospholipid/polydiacetylene colorimetric vesicle assay, *Biochemistry 39*, 15851−15859.
18. Yoshida, S., and Plant, S. (1991) A potassium current evoked by growth hormone-releasing hormone in follicular oocytes of *Xenopus laevis*, *J. Physiol. 443*, 651−667.
19. Kolusheva, S., Boyer, L., and Jelinek, R. (2000) A colorimetric assay for rapid screening of antimicrobial peptides, *Nat. Biotechnol. 18*, 225−227.
20. Rozner, S., Kolusheva, S., Cohen, Z., Dowhan, W., Eichler, J., and Jelinek, R. (2003) Detection and analysis of membrane interactions by a biomimetic colorimetric lipid/polydiacetylene assay, *Anal. Biochem. 319*, 96−104.
21. Chen, Y., Dalwadi, G., and Benson, H. A. E. (2004) Drug delivery across the blood-brain barrier, *Curr. Drug Delivery 1*, 361−376.
22. Kansy, M., Avdeef, A., and Fischer, H. (2004) Advances in screening for membrane permeability: High-resolution PAMPA for medicinal chemists, *Drug Discovery Today: Technologies 1*, 349−355.
23. Leeson, P. D., and Davis, A. M. (2004) Time-Related Differences in the Physical Property Profiles of Oral Drugs, *J. Med. Chem. 47*, 6338−6348.
24. Ouellette, A. J., and Selsted, M. E. (1996) Paneth cell defensins: endogenous peptide components of intestinal host defense, *FASEB J. 10*, 1280−1289.
25. Kleine, T. J., Lewis, P. N., and Lewis, S. A. (1997) Histone-induced damage of a mammalian epithelium: The role of protein and membrane structure, *Am. J. Physiol. 273*, C1925−C1936.
26. Harris, W. E., and Stahl, W. L. (1978) Interactions of adrenergic compounds with brain membrane constituents, *Biochem. Pharmacol. 27*, 2015−2019.
27. Jen, W. C., Jones, G. A., Brewer, D., Parkinson, V. O., and Taylor, A. (1987) The antibacterial activity of alamethicins and zervamicins, *J. Appl. Bacteriol. 63*, 293−298.
28. Kylyvnyk, K. E. (2003) Influence of substance structure on change of electrochemical properties of bilayer lipid membranes, *NATO Sci. Ser., II 95*, 255−264.
29. Yang, W., Yamauchi, A., and Kimizuka, H. (1987) Membrane potential and ion flux in a reverse transport system with a liquid membrane using monensin as a carrier, *J. Membr. Sci. 31*, 109−116.
30. Pressman, B. C. (1976) Biological applications of ionophores, *Annu. Rev. Biochem. 45*, 501−530.
31. Liesi, P., Wright, J. M., and Krauthamer, V. (1997) BAPTA-AM and ethanol protect cerebellar granule neurons from the destructive effect of the Weaver gene, *J. Neurosci. Res. 48*, 571−579.
32. Tomita, T., Hata, T., and Tokuno, H. (2000) Effects of removal and reapplication of K^+ and Cl^- on spontaneous electrical activity, slow wave, in the circular muscle of the guinea-pig gastric antrum, *Jpn. J. Physiol. 50*, 191−198.
33. Jennette, K. W. (1981) The role of metals in carcinogenesis: Biochemistry and metabolism, *Environ. Health Perspect. 40*, 233−252.
34. Anastassopoulou, J., and Theophanides, T. (1995) The role of metal ions in biological systems and medicine, *NATO Sci. Ser., Ser. C 459*, 209−218.
35. Vallee, B. L., and Falchuk, K. H. (1993) The biochemical basis of zinc physiology, *Physiol. Rev. 73*, 79−118.
36. Erdahl, W. L., Chapman, C. J., Wang, E., Taylor, R. W., and Pfeiffer, D. R. (1996) Ionophore 4-BrA23187 Transports Zn^{2+} and Mn^{2+} with High Selectivity Over Ca^{2+}, *Biochemistry 35*, 13817−13825.

BI050718X